

晚更新世长江中下游沙山和黄土物质来源研究

林 旭^{1,2*}, 刘海金³, 陈济鑫¹, 李玲玲¹, 胡程伟¹, 张玉芬⁴, 李长安⁵

1. 三峡大学 土木与建筑学院, 宜昌 443002

2. 三峡库区地质灾害教育部重点实验室(三峡大学), 宜昌 443002

3. 东华理工大学 地球科学学院, 南昌 330013

4. 中国地质大学(武汉) 地球物理与空间信息学院, 武汉 430078

5. 中国地质大学(武汉) 地理与信息工程学院, 武汉 430078

摘要: 风成沉积物的产生、搬运和沉积过程是地球各圈层相互作用的产物。晚更新世末次冰期时, 长江中下游广泛分布沙山和黄土, 对于它们是远源搬运而来, 还是近源堆积一直存有争议。对青山、九江、定山和红光这些典型沙山和黄土剖面进行碎屑锆石 U-Pb 年龄分析, 获得 346 个新数据结果, 将其与潜在物源区的碎屑锆石 U-Pb 年龄进行对比, 结合这些地层的沉积时代和区域内已报道的物源示踪结果, 发现在末次冰期青山沙山和九江黄土的碎屑锆石来自近源的江汉平原, 定山沙山和红光黄土的碎屑锆石来自赣江。长江中下游沙山和黄土的发育属于河流搬运的碎屑物质被东亚冬季风吹拂和高大地形阻挡发生沉积的模式。

关键词: 沙山; 黄土; 长江; 锆石 U-Pb 年龄; 物源示踪

Provenance tracing of sand hills and loess in the middle and lower reaches of Yangtze River during the Late Pleistocene

LIN Xu^{1,2*}, LIU Haijin³, CHEN Jixin¹, LI Lingling¹, HU Chengwei¹, ZHANG Yufen⁴, LI Chang'an⁵

1. School of Civil Engineering and Architecture, China Three Gorges University, Yichang 443002, China

2. Key Laboratory of Geological Hazards on Three Gorges Reservoir Area, Ministry of Education, China Three Gorges University, Yichang 443002, China

3. School of Earth Sciences, East China University of Technology, Nanchang 330013, China

4. School of Geophysics and Spatial Information, China University of Geosciences, Wuhan 430078, China

5. School of Geography and Information Engineering, China University of Geosciences, Wuhan 430078, China

Abstract: *Background, aim, and scope* The generation, transport, and deposition of eolian sediments are the result of the interaction between the Earth's atmosphere, hydrosphere, and lithosphere. The last period of prolonged and frequent climatic fluctuations occurred during the last glaciation of the Late Pleistocene (75—10 ka). Therefore, provenance tracing of well-preserved deserts or loess, reconstructing their transportation paths, and understanding the climatic characteristics of this period have important significance for the future

收稿日期: 2021-10-25; 录用日期: 2022-02-02; 网络出版: 2022-02-20

Received Date: 2021-10-25; **Accepted Date:** 2022-02-02; **Online first:** 2022-02-20

基金项目: 国家自然科学基金项目(41877292, 41871019, 41972212)

Foundation Item: National Natural Science Foundation of China (41877292, 41871019, 41972212)

通信作者: 林 旭, E-mail: hanwiji-life@163.com

Corresponding Author: LIN Xu, E-mail: hanwiji-life@163.com

引用格式: 林 旭, 刘海金, 陈济鑫, 等. 2022. 晚更新世长江中下游沙山和黄土物质来源研究 [J]. 地球环境学报, 13(5): 529—542.

Citation: Lin X, Liu H J, Chen J X, et al. 2022. Provenance tracing of sand hills and loess in the middle and lower reaches of Yangtze River during the Late Pleistocene [J]. Journal of Earth Environment, 13(5): 529—542.

development of human society. During the last glacial period of the Late Pleistocene, sand hills and loess were widely distributed in the middle and lower reaches of Yangtze River. Some researchers believe that they originated from the Gobi Desert and loess from Mongolia and northern China, while others speculate that they were derived from the adjacent provenance area. Thus, the origin of these eolian sediments remains controversial. In this study, we conducted detrital zircon U-Pb age analysis from the continuous distribution, and well-exposed sand hills and loess profiles along the middle and lower reaches of Yangtze River. We simultaneously collected published detrital zircon U-Pb ages from the Gobi Desert and loess of Mongolia and northern China, the Yangtze River Basin, and the Jianghan Plain. In this study, the specific source regions of the sand hills and loess were determined based on a comparison of the detrital zircon U-Pb age spectrum and the published provenance tracing results in the region. **Materials and methods** Four detrital samples were analyzed for zircon U-Pb ages from the Qingshan and Dingshan sand hills, Jiujiang, and the Hongguang loess distributed in the middle and lower reaches of Yangtze River. Non-metric multidimensional scaling (MDS) maps were used to visualize the similarities and diversity of complex zircon age distributions. **Results** The analyzed zircons were mainly magmatic. We obtained 346 new zircon U-Pb ages, and the detrital zircon U-Pb ages of the Qingshan sand hill showed five main peaks: 212 Ma, 427 Ma, 786 Ma, 915 Ma, and 1855 Ma. The detrital zircon U-Pb age compositions of the Jiujiang loess are Mesozoic (204 Ma), Early Paleozoic (434 Ma), Neoproterozoic (778 Ma and 958 Ma), Paleoproterozoic (1719 Ma and 1841 Ma), and Neoarchean (2530 Ma). The detrital zircon U-Pb ages of the Dingshan sand hill show Late Mesozoic (126 Ma), Early Mesozoic (219 Ma), Early Paleozoic (449 Ma), Neoproterozoic (822 Ma and 980 Ma), and non-significant Paleoproterozoic (1891 Ma) peak ages. The detrital zircon U-Pb peak ages of the Hongguang loess include 140 Ma, 211 Ma, 420 Ma, 807 Ma, and 980 Ma, but the Paleoproterozoic (1755 Ma) and Neoarchean (2466 Ma) peak ages were not significant. **Discussion** The comparison of the results shows that the detrital zircon U-Pb age spectra of the Qingshan sand hill and Jiujiang loess are consistent with that of the Jianghan Plain. The detrital zircon U-Pb age compositions of the Dingshan sand hill and Hongguang loess were similar to those of the Ganjiang River. However, they differ from the detrital zircon U-Pb age compositions of the Gobi Desert and loess in Mongolia and northern China. Combined with the MDS plot, the Qingshan sand hill and Jiujiang loess were close to the Jianghan Plain, whereas the Dingshan sand hill and Hongguang loess are closely related to the Ganjiang River. Previously published grain size studies have indicated that these are eolian sediments. During the last glacial period, the continental shelf in the eastern China sea retreated, thereby exposing the detrital material of the Jianghan Plain and Ganjiang River. The East Asian winter monsoon strengthened during this period. Blown by the East Asian winter monsoon, exposed debris was transported and deposited in the northern piedmont of the orogenic belts along the middle and lower reaches of Yangtze River. The provenance tracing results also indicate that the sand hills and loess distributed in the middle and lower reaches of Yangtze River are mainly near source materials. In contrast, the influences of the Gobi Desert and loess in Mongolia and northern China were not dominant. **Conclusions** By analyzing the detrital zircon U-Pb ages of the sand hills and loess from the middle and lower reaches of Yangtze River, and comparing them with the potential provenance areas, we found that the detrital zircons from the Qingshan sand hill, Jiujiang loess, Dingshan sand hill, and Hongguang loess were mainly derived from the Jianghan Plain and Ganjiang River during the last glacial period. The development of sand hills and loess in the middle and lower reaches of Yangtze River are derived by the model of river-transported detritus, which was blown by East Asian winter monsoon and blocked by tall topography for deposition. **Recommendations and perspectives** Although detrital zircons provided reliable results in this study, it is necessary to combine various methods to comprehensively display provenance tracing results for the sand hills and loess in the middle and lower reaches of Yangtze River in the future.

Key words: sand hill; loess; Yangtze River; zircon U-Pb age; provenance tracing

沙漠、黄土的沉积过程是地球各圈层相互作用的产物 (An et al, 2001; 孙继敏, 2020; Sun et al, 2020)。晚更新世末次冰期 (75—10 ka) 是离人类最近的一次持续时间长、气候波动频繁的时期 (Hou et al, 2017; Xie et al, 2018; Windler et al, 2021)，对保存良好的沙漠或黄土开展从源到汇的研究，限定这些粉尘的源区，重建它们的搬运路径，从而了解这个时期的气候特征，对人类社会未来发展具有重要的地质历史借鉴意义。

长江中下游是我国经济发达、人口密集的区域，从“人地关系论”的角度出发，气候的波动变化直接影响到该区域的社会经济发展。2021年3月15日，发源于蒙古国南部的沙尘暴扩散到我国内蒙古、河北西北部一带 (Filonchyk, 2021; Yin et al, 2021; Liang et al, 2022)。在2017年

5月5日，沙尘暴波及范围甚至达到长江流域 (图1)，对区域内的工农业生产造成直接危害，由此形成的沙尘气溶胶通过多种途径对环境、生态、气候和人体健康等多方面造成滞后、持续、长期的间接危害 (杨晓军等, 2021; Han et al, 2021)。晚更新世末次冰期时，长江中下游广泛分布沙山和黄土，它们是否和蒙古、我国北方的戈壁、沙漠和黄土有物源联系？从以往的研究结果来看，有研究者认为这些风成沉积物属于远源成因 (刘东生, 1985; 李徐生等, 2001)，即来自我国北方，也有人认为是近源成因 (杨勇等, 2008; Hao et al, 2010)。因而，限定长江中下游晚更新世沙山和黄土的物源区，是厘定上述争论的关键，也是从“将古论今”的角度讨论长江流域现今人地关系发展的重要步骤。



本图基于自然资源部标准地图服务网 (<http://bzdt.ch.mnr.gov.cn/>) 下载的审图号为 GS(2016)1594 号的标准地图制作，底图无修改。

图1 2017年5月5日沙尘暴天气预报图 (根据中央气象台 (<http://www.nmc.cn/>) 发布数据绘制)
Fig. 1 Sandstorm weather forecast on May 5, 2017
(modified from China Central Meteorological Observatory (<http://www.nmc.cn/>))

碎屑锆石是沙山和黄土沉积物中广泛存在的矿物，同时也是开展原位 U-Pb 定年的理想矿物，被广泛用于我国北方风成沉积物的物源示踪研究 (Zhang et al, 2016; Sun et al, 2018; Fan et al, 2019; 林旭等, 2021a; Zhang et al, 2021)。长江中下游黄土的碎屑锆石 U-Pb 年龄研究见于镇江下蜀黄土 (Liu et al, 2014; Wang et al, 2018)、

长江三角洲下蜀黄土 (Qian et al, 2018; Wu et al, 2021)。而长江中游江汉盆地、下游鄱阳湖周围的沙山和黄土的碎屑锆石 U-Pb 年龄研究目前未见报道。因而，本文选择长江中下游分布连续、出露良好的末期冰期沉积的青山沙山、九江黄土、定山沙山、红光黄土开展碎屑锆石 U-Pb 年龄分析，同时系统搜集蒙古国和我国北方戈壁、沙漠和黄

土, 以及长江流域、江汉平原的碎屑锆石 U-Pb 年龄, 用于潜在物源区对比研究, 系统判定这些沙山和黄土的物源区, 与长江下游镇江和三角洲已开展的黄土碎屑锆石 U-Pb 年龄物源示踪结果进行对比, 重建末次冰期以来长江中下游的地貌演化格局。

1 研究区概况

江汉平原位于湖北省中南部, 西起宜昌、东迄武汉, 北抵钟祥、南临洞庭湖畔(图 2a), 介于东经 $111^{\circ}45'—114^{\circ}16'$ 、北纬 $29^{\circ}26'—31^{\circ}10'$, 面积约 $3.2 \times 10^4 \text{ km}^2$ 。江汉平原内水系发育, 长江自西向东在宜昌进入江汉平原, 汉江自北向南在钟祥进入江汉平原, 这两条河流是江汉平原最主要的输沙河流(林旭和刘静, 2019)。晚更新世时($126—10 \text{ ka}$), 江汉平原自下而上沉积了沙砾层、沙—粉沙、黏土质粉沙—粉沙质黏土, 颜色以灰黄、褐黄为主(顾延生等, 2018)。此时江汉平原受全球冰期-间冰期气候变化的影响, 经历了寒冷(早期)→温湿(中期)→寒冷(晚期)的气候旋回(张玉芬等, 2016)。与此同时, 我国东部陆架海的海平面发生大幅度下降, 导致大陆架大面积出露, 出现沙漠化现象(赵松龄, 1996)。在江汉盆地、鄱阳湖盆地, 以及湖口以东的长江沿岸则分布面积广大的沙山和黄土(杨达源, 1986)。这些沙山的高度一般在 $10—70 \text{ m}$, 最高可达 140 m (林承坤, 1959; 景存义和邱淑彭, 1980; 杨达源, 1985)。

2 样品采集

武汉市青山镇江边的沙山呈条带状与长江近似平行展布, 沙层厚 $10—50 \text{ m}$ 。此次开展采样的剖面高约 20 m ($114^{\circ}24'56''\text{E}, 30^{\circ}39'20''\text{N}$), 位于长江河道二级阶地上。采样点位于杨勇等(2008)开展粒度分析的沙山顶部深约 2.8 m 的沙层中。所在层位的年龄根据和同期湖口柘矶沙山(吴艳宏等, 2000; 桑亚伟, 2020)、定山沙山(贾玉芳, 2012)进行对比, 确定为末次冰期。定山镇沙山剖面位于长江南岸 214 省道旁($116^{\circ}26'00''\text{E}, 29^{\circ}51'23''\text{N}$), 高度在 60 m 左右, 未见底。采样点位于贾玉芳(2012)开展粒度分析的剖面顶部, 沉积时代为末次冰期(17.9 ka)。九江黄土剖面位于长虹大道北部的南湖公园内($116^{\circ}00'38''\text{E}, 29^{\circ}42'27''\text{N}$), 采样点位于剖面顶部约 2 m 处, 属于褐黄色泥质粉沙

黄土, 固结程度较好, 块状构造, 含少量铁锰胶膜, 其沉积特征与蒋复初等(1997)的描述相似, 确定沉积时代为末次冰期(49 ka)。红光黄土剖面位于彭泽县定山镇红光小学以东 2 km 公路旁($116^{\circ}26'02''\text{E}, 29^{\circ}50'38''\text{N}$), 采样点位于剖面中部, 地层沉积时代介于 $56—67 \text{ ka}$ (Lai et al, 2010)。剖面中的黄土具有块状构造, 垂直节理发育, 质地致密。

3 实验方法

首先将 3 kg 左右的样品经过淘洗、电磁仪分离后, 在双目镜下随机挑选出约 1000 粒锆石颗粒。然后将约 200 颗锆石用环氧树脂固定并抛光, 露出锆石晶面。再经过反射光和透射光照相后, 进行阴极发光(CL)照相, 以了解锆石的外部情况和内部结构。锆石 U-Pb 同位素定年在南京宏创地质勘查技术服务有限公司微区分析实验室使用激光剥蚀-电感耦合等离子体质谱仪(LA-ICPMS)完成。激光剥蚀平台采用 Resolution SE 型 193 nm 深紫外激光剥蚀进样系统, 配备 S155 型双体积样品池。质谱仪采用 Agilent 7900 型电感耦合等离子体质谱仪。采用 5 个激光脉冲对每个剥蚀区域进行预剥蚀(剥蚀深度约 $0.3 \mu\text{m}$), 在束斑直径 $30 \mu\text{m}$ 、剥蚀频率 5 Hz 、能量密度 $2 \text{ J}\cdot\text{cm}^{-2}$ 的激光条件下分析样品。锆石 91500 作为校正标样, GJ-1 作为监测标样, 每隔 $10—12$ 个样品点分析 2 个 91500 标样及 1 个 GJ-1 标样。通常采集 20 s 的气体空白, $35—40 \text{ s}$ 的信号区间进行数据处理。以 NIST 610 作为外标, ^{91}Zr 作为内标计算微量元素含量。选择 $^{206}\text{Pb}/^{238}\text{U}$ (年龄 $<1000 \text{ Ma}$) 或 $^{207}\text{Pb}/^{206}\text{Pb}$ (年龄 $>1000 \text{ Ma}$) 谐和度在 $90\%—99\%$ 的年龄结果。锆石 U-Pb 年龄频率分布图采用 DensityPlotter 软件完成(Vermeesch, 2012)。使用 IsoplotR 软件可以有效实现多维尺度(MDS)判别, 实现样品的相似/相异分析(Vermeesch, 2018)。根据输出图中相似样品紧密聚集在一起, 而不同样品相距很远, 结合锆石 U-Pb 年龄谱对比结果, 可以辅助判别物源区。

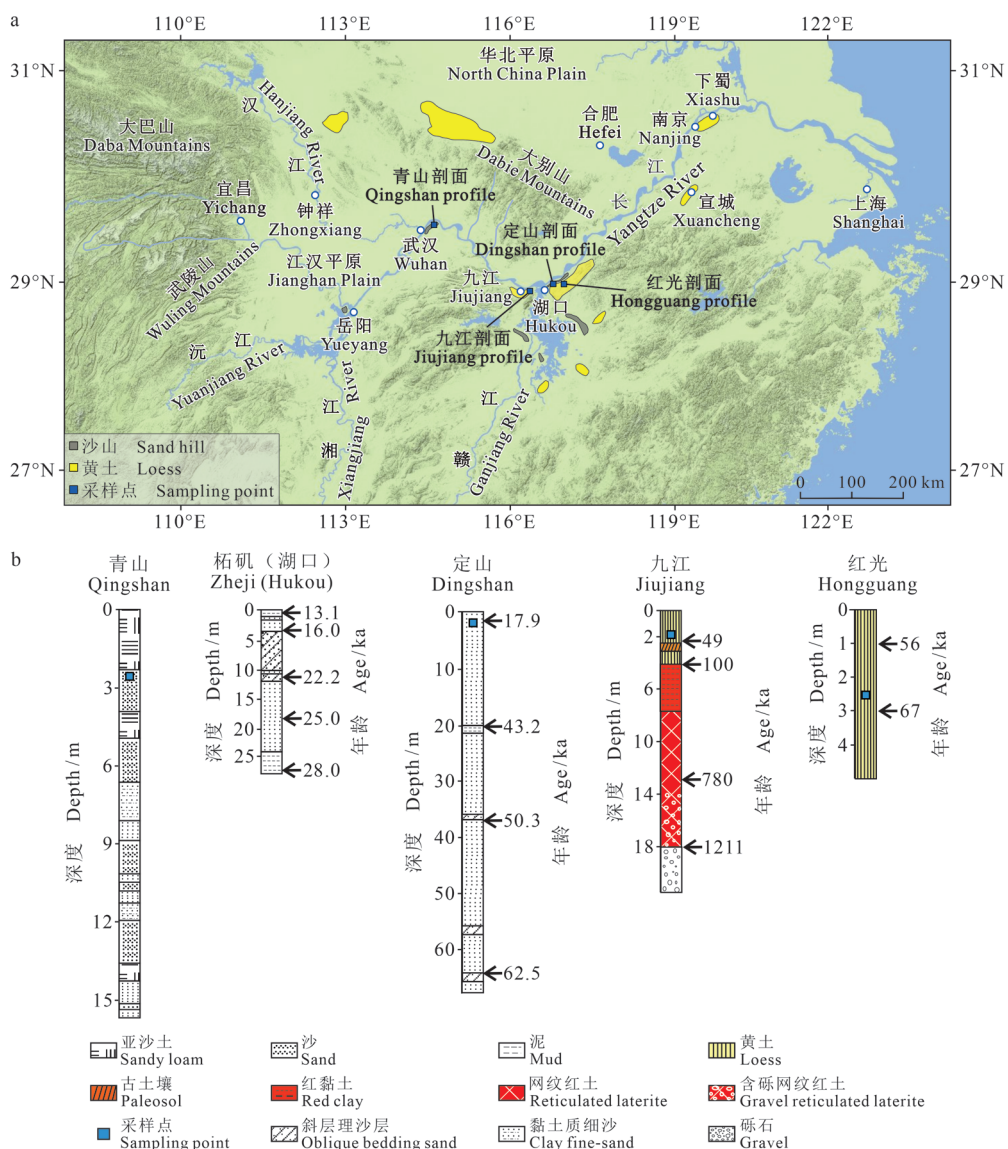
4 实验结果

此次分析的锆石主要为长柱状、棱柱状和半自形短柱状。阴极发光图像清晰显示锆石的内部结构, 主要以具有典型震荡环带的岩浆锆石为主。此外, 锆石中的 Th、U 含量及 Th/U 比值与锆石

的成因有关。一般而言, 岩浆锆石中 Th、U 含量较高, Th/U 值 >0.4 ; 变质锆石中 Th、U 含量低, Th/U 值 <0.1 。此次分析的锆石有 346 颗, 除 6 颗锆石的 Th/U 值 <0.1 外, 其余锆石大都是岩浆来源。

青山沙山的碎屑锆石 U-Pb 年龄出现 212 Ma、427 Ma、786 Ma、915 Ma 和 1855 Ma 5 个主要峰值(图 6a)。九江黄土碎屑锆石 U-Pb 年龄组成由中生代(204 Ma)、早古生代(434 Ma)、新元

古代(778 Ma 和 958 Ma)、古元古代(1719 Ma 和 1841 Ma)和新太古代(2530 Ma)组成。定山沙山的碎屑锆石 U-Pb 年龄出现晚中生代(126 Ma)、早中生代(219 Ma)、早古生代(449 Ma)、新元古代峰值(822 Ma 和 980 Ma), 以及不显著的古元古代峰值(1891 Ma)。红光黄土的碎屑锆石 U-Pb 峰值年龄包含: 140 Ma、211 Ma、420 Ma、807 Ma、980 Ma, 其古元古代(1755 Ma)和新太古代(2466 Ma)峰值年龄不显著。

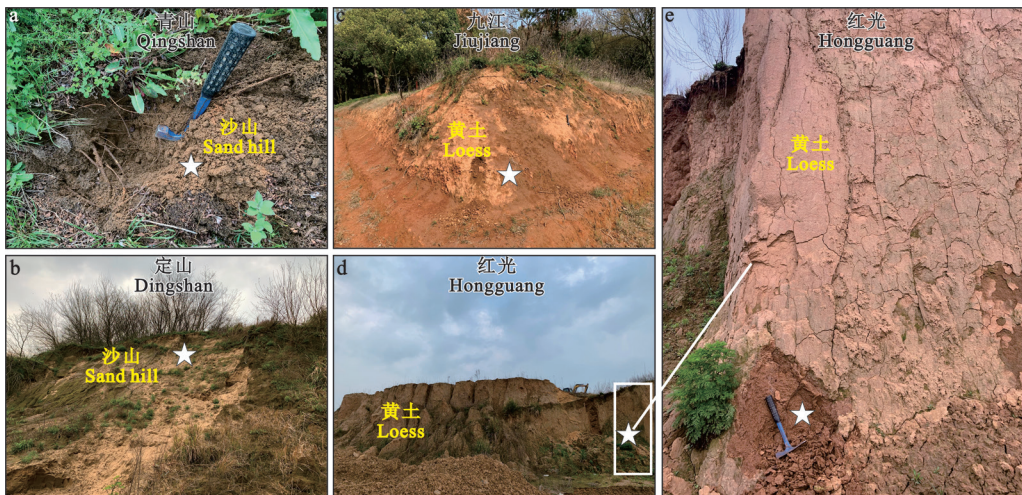


青山沙山(杨勇等, 2008)、柘矶沙山(贾玉芳, 2012)、定山沙山(贾玉芳, 2012)、九江黄土(蒋复初等, 1997)、红光黄土(Lai et al., 2010)。

Qingshan sand hill (Yang Y et al, 2008), Zheji sand hill (Jia Y F, 2012), Dingshan sand hill (Jia Y F, 2012), Jiujiang loess (Jiang F C et al, 1997), Hongguang loess (Lai et al, 2010).

图 2 长江中下游沙山和黄土分布图(a), 典型沙山和黄土柱状图(b)

Fig. 2 Distribution of sand hills and loess in the middle and lower reaches of Yangtze River (a), typical sand hill and loess histogram (b)



a: 青山沙山, b: 定山沙山, c: 九江黄土, d、e: 红光黄土。图中五角星代表具体的采样位置。

a: Qingshan sand hill, b: Dingshan sand hill, c: Jiujiang loess, d and e: Hongguang loess. The pentagram in the figure represents the specific sampling location.

图 3 野外样品采集照片
Fig. 3 Photos of field sample collection

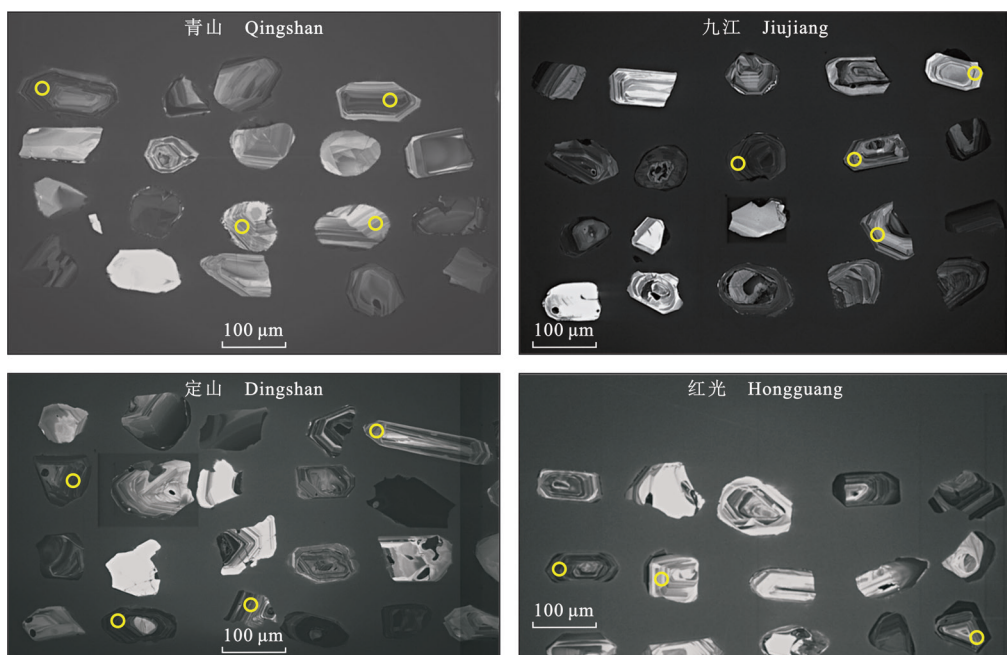


图 4 锆石阴极发光图 (圆圈代表样品测试点)
Fig. 4 Cathodoluminescence pictures of zircon grains (circles representing sample analysis points)

5 讨论

5.1 长江中下游沙山和黄土在末次冰期来自近源物质

通过对比可以发现: 青山沙山(图 7a)、九江黄土(图 7c)和江汉平原的碎屑锆石 U-Pb 峰值年龄组成相似(He et al., 2013; Liang et al.,

2018; 图 7b)。塔里木盆地中的塔克拉玛干沙漠的碎屑锆石 U-Pb 峰值年龄(谢静等, 2007; Rittner et al., 2016; 图 7h)存在明显的晚古生代(283 Ma)和早古生代(449 Ma)峰值年龄, 这与我国北方戈壁的碎屑锆石 U-Pb 峰值年龄组成相似(Che and Li, 2013; Zhang et al., 2016), 但二者的新元古代和古元古代峰值年龄不显著(图

7i)。包括巴丹吉林沙漠 (Zhang et al, 2016)、腾格里沙漠 (Zhang et al, 2016; Fan et al, 2019)、毛乌素沙漠 (Stevens et al, 2010)、库布齐沙漠 (杨利荣等, 2017) 和科尔沁沙地 (Stevens et al, 2010; Xie et al, 2012) 在内的我国北方沙漠 (图 7j) 的碎屑锆石 U-Pb 峰值年龄组成和黄土高原相似 (Stevens et al, 2010; Pullen et al, 2011; Nie et al, 2014; 图 7k), 但中生代峰值年龄均不是二者的主导峰值, 这与青山沙山和九江截然不同。华北平原位于华北克拉通内部, 其锆石 U-Pb 年龄组成 (图 7l) 与上述所有地区相比, 最大的特征是新元古代峰值年龄不显著 (林旭等, 2021b)。结合 MDS 判定结果 (图 8), 可以发现青山沙山、九江黄土与江汉平原的距离较近, 而与塔里木盆地、我国北方戈壁、沙漠和黄土高原的距离较远。这进一步说明青山沙山、九江黄土与江汉平原的锆石具有物源联系。定山沙山 (图 7e) 和红光黄土 (图 7g) 的碎屑锆石 U-Pb 年龄组成与江汉平原 (图 7b) 和湖口到铜陵段长江 (He et al, 2013) 相比 (图 7d), 其具有晚中生代峰值年龄 (126 Ma 和 140 Ma), 同时古元古代和新太古代峰值年龄不显著。赣江是鄱阳湖最大的输沙河流, 其下游碎屑锆石 U-Pb 年龄无论是频率分布

形态还是峰值组成 (He et al, 2013; 李小聪等, 2016; 图 7f), 都与定山沙山和红光黄土具有相似性。在更大的区域上对比, 可以发现定山沙山和红光黄土的碎屑锆石 U-Pb 年龄组成和塔里木盆地、我国北方戈壁、沙漠和黄土高原相比, 最主要的特征在于其出现中生代峰值年龄。因此, 二者之间不具有物源联系。在 MDS 判定图中 (图 8), 定山沙山、九江黄土与赣江的距离相近, 而与江汉平原和长江的距离较远, 进一步说明定山沙山、九江黄土与赣江之间的锆石具有物源联系。

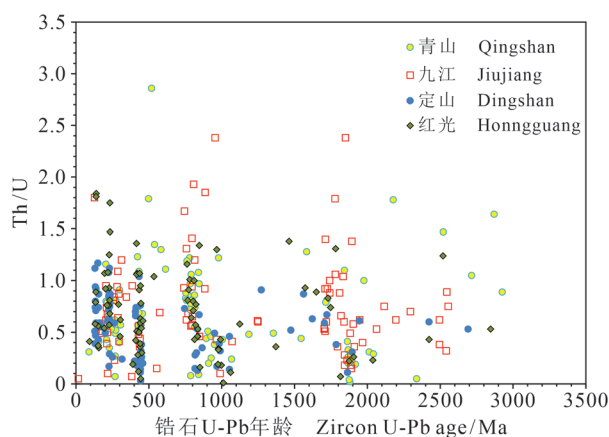


图 5 锆石 U-Pb 年龄与 Th/U 比值散点图

Fig. 5 Scatter plot of zircon U-Pb age and Th/U ratio

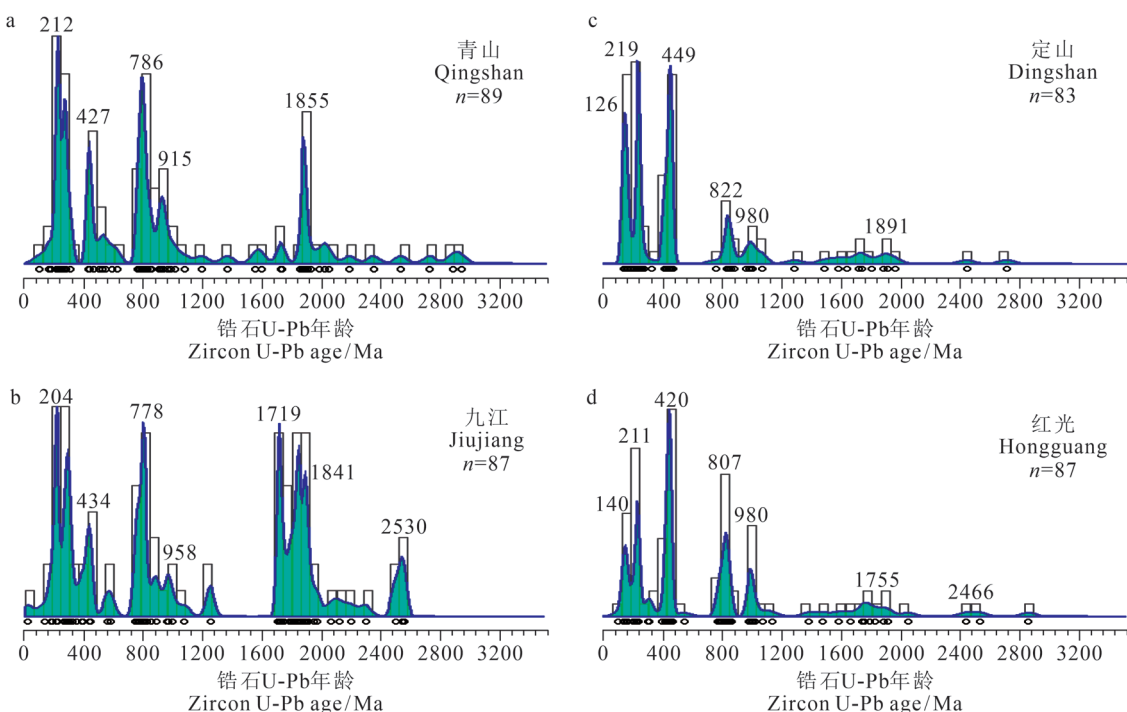
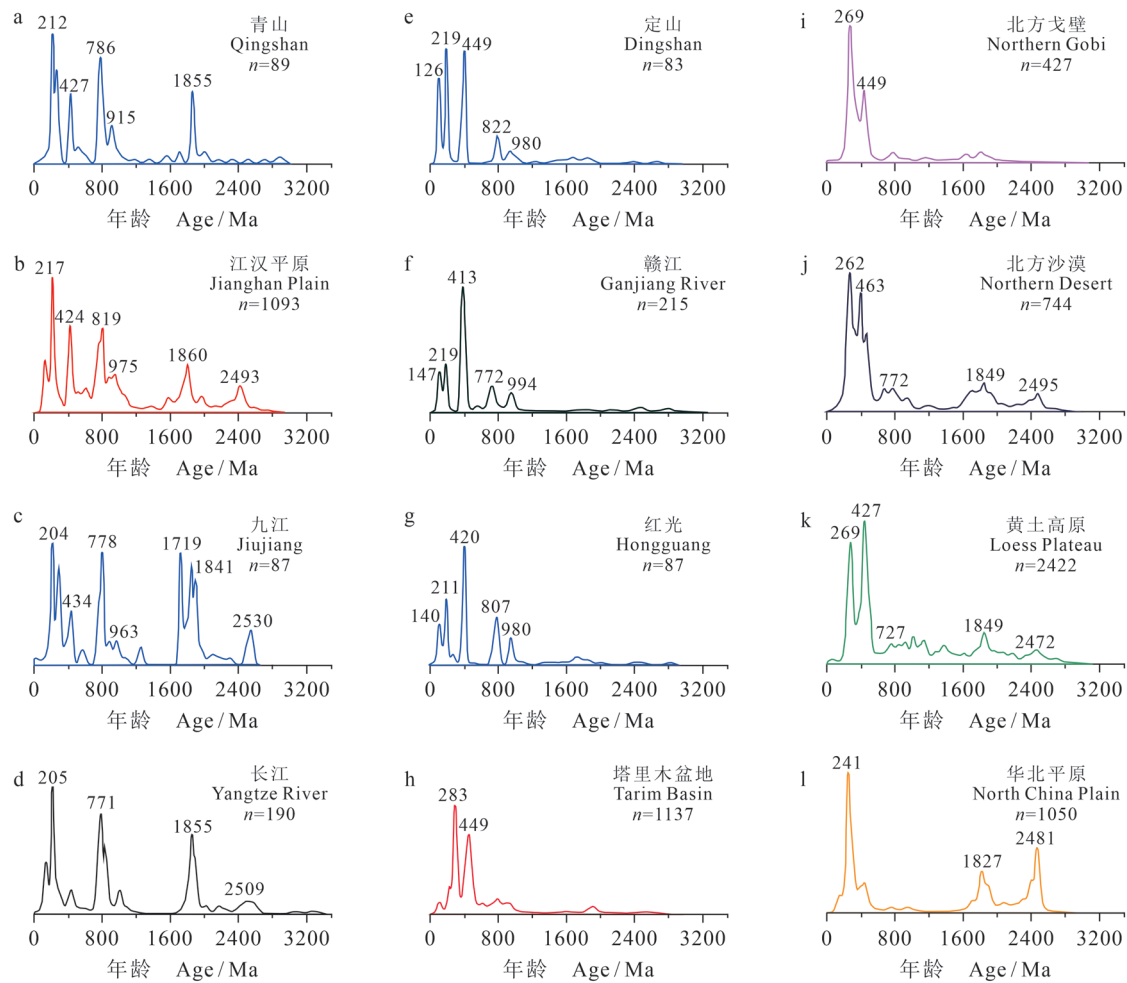


图 6 锆石 U-Pb 年龄组成分布图
Fig. 6 Zircon U-Pb age composition distribution diagram



江汉平原 (He et al., 2013; Liang et al., 2018), 长江 (He et al., 2013), 赣江 (He et al., 2013; 李小聪等, 2016), 塔里木盆地 (谢静等, 2007; Rittner et al., 2016), 北方戈壁 (Che and Li, 2013; Zhang et al., 2016), 北方沙漠 (Stevens et al., 2010; Xie et al., 2012; Zhang et al., 2016; 杨利荣等, 2017; Fan et al., 2019), 黄土高原 (Stevens et al., 2010; Pullen et al., 2011; Nie et al., 2014), 华北平原 (林旭等, 2021b)。

Jianhan Plain (He et al., 2013; Liang et al., 2018), Yangtze River (He et al., 2013), Ganjiang River (He et al., 2013; Li X C et al., 2016), Tarim Basin (Xie J et al., 2007; Rittner et al., 2016), the Northern Gobi (Che and Li, 2013; Zhang et al., 2016), Northern Desert (Stevens et al., 2010; Xie et al., 2012; Zhang et al., 2016; Yang L R et al., 2017; Fan et al., 2019), Loess Plateau (Stevens et al., 2010; Pullen et al., 2011; Nie et al., 2014), North China Plain (Lin X et al., 2021b).

图 7 锆石 U-Pb 年龄

Fig. 7 Zircon U-Pb ages

粒度分析结果表明: 青山沙山 (杨勇等, 2008) 和九江黄土 (李敬卫等, 2009)、定山沙山 (贾玉芳, 2012) 和红光黄土 (胡亚萍等, 2013) 都属于风成沉积物。青山沙山的物源示踪结果至今未有报道, 但全岩地球化学物源示踪结果表明九江黄土的物质主要来自近源的长江物质 (凌超豪等, 2018; Zhang and Jia, 2019)。定山沙山 (张智, 2013) 和红光黄土 (Jia et al., 2012) 的物源示踪结果表明其主要受长江和赣江的物质影响。林承坤 (1959) 通过详细的野外剖

面考察后, 发现长江和赣江自中更新世以来存在多次河道摆动现象。尽管现在定山沙山和红光黄土位于长江干流南岸, 但在晚更新世长江干流位于其现在河道更北面, 而赣江河道位于现今长江的位置 (林承坤, 1959)。所以, 晚更新世末次冰期时, 受干冷气候的影响, 江汉平原内的长江和汉江, 以及鄱阳湖平原内的赣江等河流水位下降, 导致江汉平原和鄱阳湖平原内水体面积和水位大幅度减小和下降, 而松散的河床碎屑沉积物广泛出露。因而, 在东亚冬季风的吹拂下, 青山

沙山和九江黄土、定山沙山和红光黄土的碎屑锆石在末次冰期分别来自近源的江汉平原和赣江。

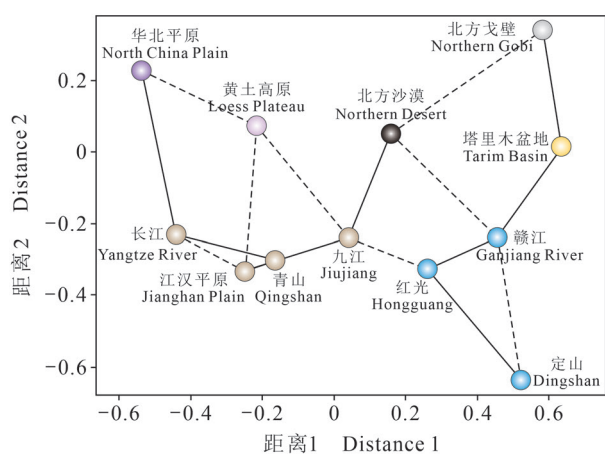


图8 锆石U-Pb年龄MDS判定图
Fig. 8 Zircon U-Pb age MDS determination diagram

全岩地球化学物源示踪和粒度分析结果表明: 长江下游北岸的晚更新世黄土来自近源的淮河河漫滩 (Han et al., 2019; Jiang et al., 2020), 而长江南岸宣城则主要受长江干涸河床松散物质的影响 (Hao et al., 2010; Qiao et al., 2011)。锆石U-Pb年龄 (Liu et al., 2014; Wu et al., 2021)、全岩Sr-Nd (Zhu et al., 2021) 和微量元素 (綦琳等, 2020) 物源示踪结果揭示长江下游南京附近的晚更新世黄土以近源长江河漫滩物质为主, 蒙古和我国北方沙漠、戈壁和黄土的影响居于次要位置。全岩地球化学和碎屑锆石U-Pb年龄物源示踪结果证实长江三角洲的晚更新世黄土以近源长江河漫滩物质为主 (Qian et al., 2018)。因而, 长江中下游晚更新世广泛分布的沙山和黄土沉积物主要来自近源物源区。

5.2 晚更新世长江中下游沙山和黄土堆积的地质意义

大面积和厚层风成沉积物的出现应同时具备三个主要条件 (刘东生, 1985): (1) 松散的碎屑物质供给区, (2) 强劲的地表风, (3) 良好的地形条件。首先, 晚更新世末次冰期以来, 全球气候特征以冰期-间冰期交替变化为主要特征, 引起全球海平面大规模升降变化。在末次冰盛期我国东部陆架海的海平面下降了130—150 m (Yokoyama et al., 2000), 而在末次冰期时也下降了60—80 m (Waelbroeck et al., 2002)。受此

影响, 类似现今东海海水顶托长江口河水的现象不复存在 (赵松龄, 1996; 图9)。一方面, 长江深入我国东部陆架海的距离要比间冰期长, 甚至发生海退现象; 另一方面, 受流域内东亚夏季风减弱的整体影响, 长江河床内的水位显著下降 (甚至发生断流), 这导致长江中下游平原先前被河水覆盖的地表开始大面积裸露 (林承坤, 1959; 杨达源, 1985)。其次, 晚更新世末次冰期时, 北极的冰盖体积明显增大, 并不断向南部低纬地区推进, 导致极地高压南推, 增强了西伯利亚和蒙古高压, 从而使东亚冬季风处于显著增强阶段 (刘东生, 1985)。再者, 长江下游的水文地貌特征与黄河下游出三门峡后可以向南或向北自由摆动不同, 其主要流动在大别山和九华山之间, 河道被严格约束。大别山和江南造山带在中生代和新生代经历强烈的隆升后, 第四纪时其基本的地貌轮廓已奠定 (林旭和刘静, 2019), 平均海拔超过1000 m, 这一高度可以有效拦截近地表的风沙搬运。另外, 来自我国北方的东亚冬季风在越过秦岭-大别山后, 由于远离起风地 (西伯利亚和蒙古), 其风力势必减弱 (图10)。因而, 在末次冰期时来自北方的东亚冬季风吹拂江汉平原、鄱阳湖平原和长江下游河道内的碎屑物质堆积在附近造山带的北坡山麓前。这综合体现了大气圈、水圈和岩石圈的共同作用, 导致这些风成沉积物的广泛出现。

尽管现今来自蒙古和我国北方的沙尘暴物质可以搬运到我国华南地区, 但这部分碎屑物质主要以细颗粒 (<5 μm) 悬浮式搬运为主 (孙继敏, 2020), 而青山沙山 (杨勇等, 2008) 和九江黄土 (李敬卫等, 2009)、定山沙山 (贾玉芳, 2012) 和红光黄土 (胡亚萍等, 2013) 的粒度分析结果显示: 沙山 (>100 μm) 和黄土 (10—60 μm) 的粒度组成明显比北方沙尘暴悬浮物质的粒度粗。所以, 蒙古国和我国北方的沙尘暴物质并不是长江中下游沙山和黄土的主要物源区。因此, 长江中下游的沙山和黄土发育过程 (模式) 为: 早期河流搬运的大量碎屑物质堆积于盆地和河道中, 后期这些碎屑物质在东亚冬季风的吹拂下就近堆积在造山带迎风坡山麓地带。我国是世界上广泛分布沙漠和黄土的国家, 这一风成沉积物发育与演化模式还可以在我国西北天山北麓 (Li et al., 2020)、西昆仑山北麓 (Fang et al., 2002)

和祁连山北麓 (Nottebaum et al, 2015) 出现, 此外在胶东半岛和鲁中山区的北麓 (林旭等, 2021a) 及松嫩平原 (Xie et al, 2018) 也可以发现这一黄土发育模式 (图 10)。但这些山麓黄土的

分布面积较小, 一般与造山带的走向大致平行。因而在同等地质条件下, 源区碎屑物质的面积、近地表风力的强弱、适合风成沉积物堆积的场所面积都会对风成沉积物的发育规模起到重要影响。

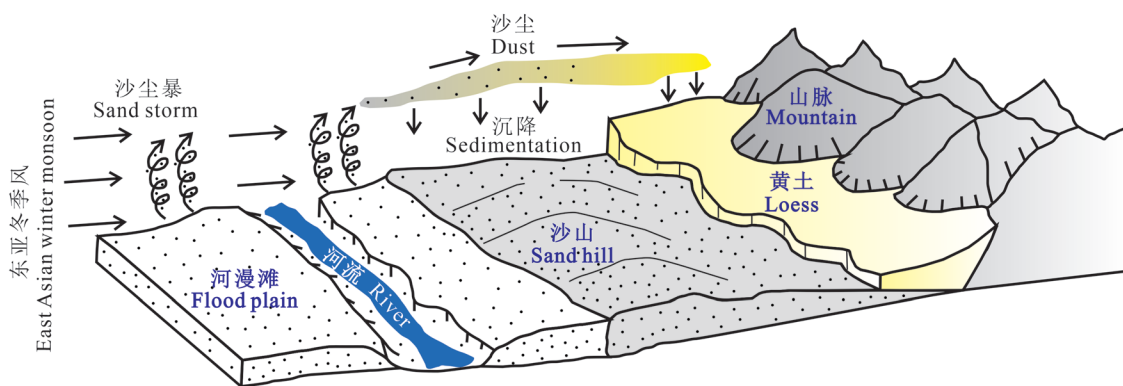


图 9 长江中下游晚更新世沙山和黄土形成模式图

Fig. 9 Formation patterns of Late Pleistocene sand hills and loess in the middle and lower reaches of Yangtze River

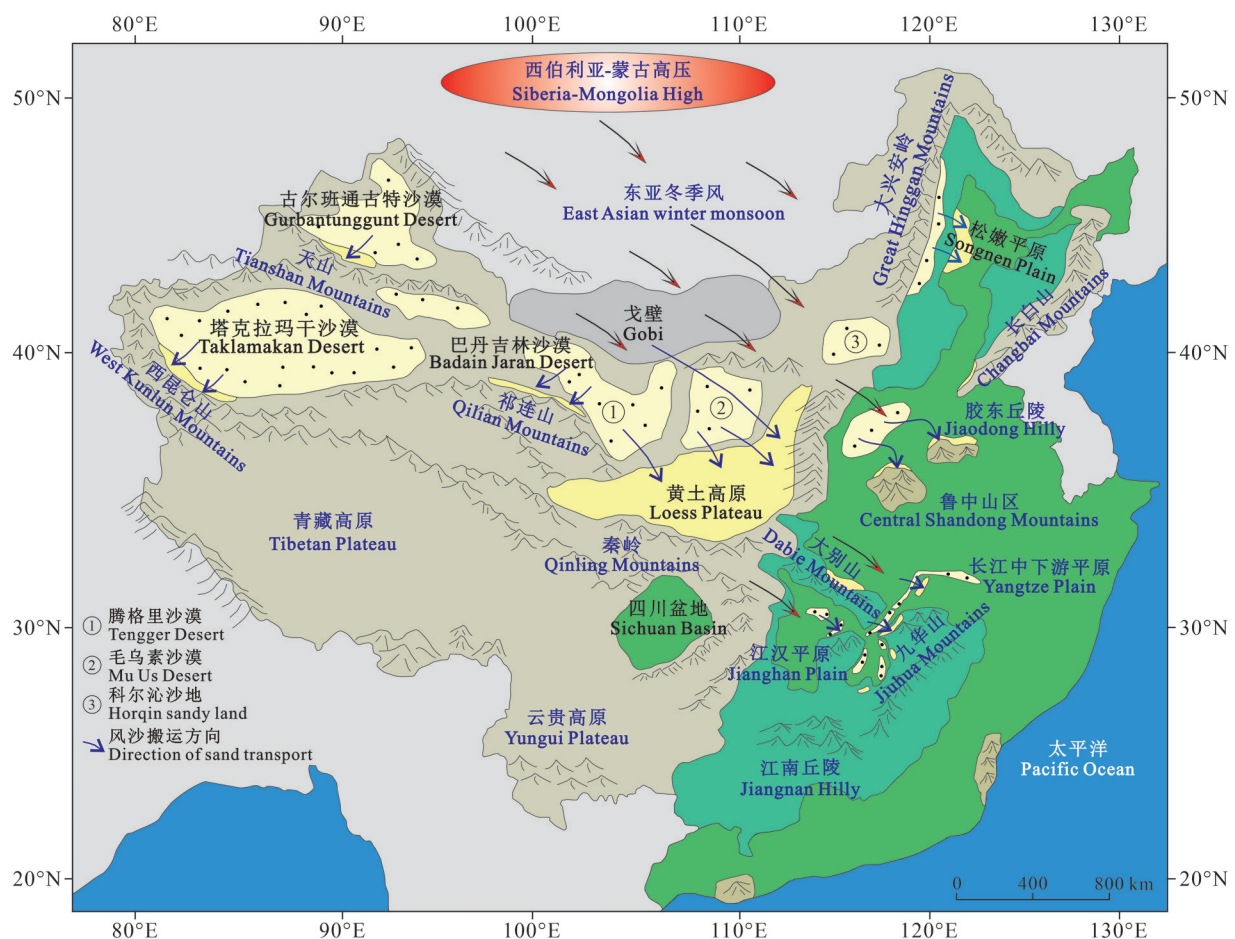


图 10 东亚晚更新世末次冰期海陆分布图

Fig. 10 Distribution of land and sea during the Last glacial period of Late Pleistocene in East Asia

6 结论

通过对长江中下游青山沙山、九江黄土、定山沙山和红光黄土进行碎屑锆石 U-Pb 年龄分析, 与潜在物源区碎屑锆石 U-Pb 年龄进行对比, 结合这些地层的沉积时代和区域内已报道的物源示踪研究结果, 得到如下结论:

(1) 青山沙山和九江黄土、定山沙山和红光黄土的碎屑锆石在末次冰期分别来自近源的江汉平原和赣江, 而与我国北方沙漠、戈壁和黄土高原没有明显的物源联系。

(2) 长江中下游沙山和黄土的发育属于河流搬运碎屑物质被东亚冬季风吹拂和高大地形阻挡发生沉积的模式。

参考文献

- 顾延生, 管 硕, 马 腾, 等. 2018. 江汉盆地东部第四纪钻孔地层与沉积环境 [J]. 地球科学, 43(11): 3989–4000.
[Gu Y S, Guan S, Ma T, et al. 2018. Quaternary sedimentary environment documented by borehole stratigraphical records in eastern Jianghan Basin [J]. *Earth Science*, 43(11): 3989–4000.]
- 胡亚萍, 贾玉连, 张 智, 等. 2013. 粒度揭示的末次间冰期以来长江中游风沙 - 风尘体系 [J]. 中国沙漠, 33(5): 1324–1332. [Hu Y P, Jia Y L, Zhang Z, et al. 2013. Sand-loess system in the middle reaches of Yangtze River since late interglacial indicated by grain size [J]. *Journal of Desert Research*, 33(5): 1324–1332.]
- 贾玉芳. 2012. 末次冰期以来鄱阳湖沙山沉积及其环境意义研究 [D]. 济南: 山东师范大学. [Jia Y F. 2012. Research on sand hills and their environmental significance in Poyang Lake region since last glacial period [D]. Jinan: Shandong Normal University.]
- 蒋复初, 吴锡浩, 肖华国, 等. 1997. 九江地区网纹红土的时代 [J]. 地质力学学报, 3(4): 27–32. [Jiang F C, Wu X H, Xiao H G, et al. 1997. Age of the vermiculated red soil in Jiujiang area, central China [J]. *Journal of Geomechanics*, 3(4): 27–32.]
- 景存义, 邱淑彰. 1980. 湖口、彭泽沿江地区第四纪地层与砂山 [J]. 南京师院学报(自然科学版), (2): 37–42, 36. [Jing C Y, Qiu S Z. 1980. Quaternary stratigraphy and sand mountain in Hukou and Pengze areas along the Yangtze River [J]. *Journal of Nanjing Normal University (Natural Science Edition)*, (2): 37–42, 36.]
- 李敬卫, 乔彦松, 王 燕, 等. 2009. 江西九江红土堆积的粒度特征及成因研究 [J]. 地质力学学报, 15(1): 95–104. [Li J W, Qiao Y S, Wang Y, et al. 2009. Aeolian origin of the red earth formation in Jiujiang City of Jiangxi Province, China: evidence from grain-size analysis [J]. *Journal of Geomechanics*, 15(1): 95–104.]
- 李小聪, 王安东, 万建军, 等. 2016. 赣江流域(南昌段)水系沉积物物源示踪研究: 来自锆石 U-Pb 同位素证据的约束 [J]. 现代地质, 30(3): 514–527. [Li X C, Wang A D, Wan J J, et al. 2016. Tracing the stream sediment of the Ganjiang River (Nanchang section): constraint from the detrital zircon U-Pb isotope evidence [J]. *Geoscience*, 30(3): 514–527.]
- 李徐生, 杨达源, 鹿化煜. 2001. 镇江下蜀黄土粒度特征及其成因初探 [J]. 海洋地质与第四纪地质, 21(1): 25–32. [Li X S, Yang D Y, Lu H Y. 2001. Grain-size features and genesis of the Xiashu loess in Zhenjiang [J]. *Marine Geology & Quaternary Geology*, 21(1): 25–32.]
- 林承坤. 1959. 第四纪古长江与沙山地形 [J]. 南京大学学报(自然科学), (2): 93–106. [Lin C K. 1959. Quaternary Yangtze River and sand mountain topography [J]. *Journal of Nanjing University (Natural Sciences)*, (2): 93–106.]
- 林 旭, 刘 静, 吴中海, 等. 2021a. 末次冰期山东黄土物源研究: 来自碎屑锆石 U-Pb 年龄的约束 [J]. 地球科学, 46(9): 3230–3244. [Lin X, Liu J, Wu Z H, et al. 2021a. Provenance of the loess in Shandong Province (eastern China) during the last ice age: constraints from the U-Pb age of detrital zircons [J]. *Earth Science*, 46(9): 3230–3244.]
- 林 旭, 刘 静, 吴中海, 等. 2021b. 环渤海湾盆地主要河流碎屑锆石 U-Pb 年龄特征及其物源示踪意义 [J]. 海洋地质与第四纪地质, 41(2): 136–145. [Lin X, Liu J, Wu Z H, et al. 2021b. U-Pb age characteristics of major fluvial detrital zircons in the Bohai Bay Basin and their provenance implications [J]. *Marine Geology & Quaternary Geology*, 41(2): 136–145.]
- 林 旭, 刘 静. 2019. 江汉和洞庭盆地与周缘造山带盆山耦合研究进展 [J]. 地震地质, 41(2): 499–520. [Lin X, Liu J. 2019. A review of mountain-basin coupling of Jianghan and Dongting basins with their surrounding mountains [J]. *Seismology and Geology*, 41(2): 499–520.]
- 凌超豪, 张 智, 贾玉连, 等. 2018. 元素地球化学揭示的长江中下游下蜀黄土物源及其环境意义 [J]. 地层学杂志,

- 42(3): 328–335. [Ling C H, Zhang Z, Jia Y L, et al. 2018. Geochemical evidence for provenance of Xiashu loess in the middle and lower reaches of the Yangtze River and its environmental implication [J]. *Journal of Stratigraphy*, 42(3): 328–335.]
- 刘东生 .1985. 黄土与环境 [M]. 北京 : 科学出版社 . [Liu T S. 1985. Loess and environment [M]. Beijing: Science Press.]
- 綦 琳, 乔彦松, 王 燕, 等 . 2020. 南京下蜀土的地球化学特征及其物源指示意义 [J]. 第四纪研究, 40(1): 190–202. [Qi L, Qiao Y S, Wang Y, et al. 2020. Geochemical characteristics of the Xiashu loess-palaeosol sequence in Nanjing and their implications for provenance [J]. *Quaternary Sciences*, 40(1): 190–202.]
- 桑亚伟 . 2020. 江西湖口地区柘矶沙山的时代、成因及气候环境意义 [D]. 北京 : 中国地质大学 (北京) . [Sang Y W. 2020. The age, origin, climatic and environmental significance of the Zheji sand hill in Hukou County, Jiangxi Province [D]. Beijing: China University of Geosciences (Beijing).]
- 孙继敏 . 2020. 黄土沉积与地球圈层相互作用 [J]. 第四纪研究, 40(1): 1–7. [Sun J M. 2020. Loess deposits and its relationship with earth sphere interactions [J]. *Quaternary Sciences*, 40(1): 1–7.]
- 吴艳宏, 羊向东, 王苏民, 等 . 2000. 九江—澎泽一带沙山研究存在问题探讨 [J]. 海洋地质与第四纪地质, 20(2): 103–106. [Wu Y H, Yang X D, Wang S M, et al. 2000. Discussion of existing problems on the research of the sand hill from Jiujiang to Pengze [J]. *Marine Geology & Quaternary Geology*, 20(2): 103–106.]
- 谢 静, 吴福元, 丁仲礼 . 2007. 浑善达克沙地的碎屑锆石 U-Pb 年龄和 Hf 同位素组成及其源区意义 [J]. 岩石学报, 23(2): 523–528. [Xie J, Wu F Y, Ding Z L. 2007. Detrital zircon composition of U-Pb ages and Hf isotope of the Hunshandake sandland and implications for its provenance [J]. *Acta Petrologica Sinica*, 23(2): 523–528.]
- 杨达源 . 1985. 江南的晚更新世风成砂丘 [J]. 中国沙漠, 5(4): 36–43. [Yang D Y. 1985. Aeolian dunes of the Late Pleistocene on south bank at the mid-lower reaches of Yangtze River [J]. *Journal of Desert Research*, 5(4): 36–43.]
- 杨达源 . 1986. 晚更新世冰期最盛时长江中下游地区的古环境 [J]. 地理学报, 41(4): 302–310. [Yang D Y. 1986. The paleoenvironment of the mid-lower regions of Changjiang in the full-glacial period of Late Pleistocene [J]. *Acta Geographica Sinica*, 41(4): 302–310.]
- 杨利荣, 邹 宁, 岳乐平, 等 . 2017. 库布齐沙漠碎屑锆石 U-Pb 年龄组成及其物源分析 [J]. 第四纪研究, 37(3): 560–569. [Yang L R, Zou N, Yue L P, et al. 2017. Distribution of U-Pb ages of detrital zircon from the Hobq Desert and its implications for provenance [J]. *Quaternary Sciences*, 37(3): 560–569.]
- 杨晓军, 张 强, 叶培龙, 等 . 2021. 中国北方 2021 年 3 月中旬持续性沙尘天气的特征及其成因 [J]. 中国沙漠, 41(3): 245–255. [Yang X J, Zhang Q, Ye P L, et al. 2021. Characteristics and causes of persistent sand-dust weather in mid-March 2021 over northern China [J]. *Journal of Desert Research*, 41(3): 245–255.]
- 杨 勇, 李长安, 胡思辉, 等 . 2008. 武汉青山“砂山”粒度特征及其成因指示 [J]. 沉积学报, 26(3): 487–493. [Yang Y, Li C A, Hu S H, et al. 2008. Grain size features and genesis of the Qingshan sand dune in Wuhan [J]. *Acta Sedimentologica Sinica*, 26(3): 487–493.]
- 张玉芬, 李长安, 孙习林, 等 . 2016. 江汉平原东北缘麻城剖面磁化率特征及气候环境意义 [J]. 地球科学, 41(7): 1225–1230. [Zhang Y F, Li C A, Sun X L, et al. 2016. Sediment magnetism characteristics and its climatic environment significance of northeast margin of Jianghan Plain [J]. *Earth Science*, 41(7): 1225–1230.]
- 张 智 . 2013. 末次间冰期以来赣北鄱阳湖地区风沙—风尘体系研究 [D]. 南昌 : 江西师范大学 . [Zhang Z. 2013. The study of sand-loess system in the Poyang Lake region since late interglacial [D]. Nanchang: Jiangxi Normal University.]
- 赵松龄 . 1996. 陆架沙漠化 [M]. 北京 : 海洋出版社 . [Zhao S L. 1996. Shelf desertification [M]. Beijing: China Ocean Press.]
- An Z S, Kutzbach J E, Prell W L, et al. 2001. Evolution of Asian monsoons and phased uplift of the Himalaya-Tibetan Plateau since Late Miocene times [J]. *Nature*, 411(6833): 62–66.
- Che X D, Li G J. 2013. Binary sources of loess on the Chinese Loess Plateau revealed by U-Pb ages of zircon [J]. *Quaternary Research*, 80(3): 545–551.
- Fan Y X, Li Z J, Wang F, et al. 2019. Provenance variations of the Tengger Desert since 2.35 Ma and its linkage with the

- northern Tibetan Plateau: evidence from U-Pb age spectra of detrital zircons [J]. *Quaternary Science Reviews*, 223: 105916. DOI: 10.1016/j.quascirev.2019.105916.
- Fang X M, Lü L Q, Yang S L, et al. 2002. Loess in Kunlun Mountains and its implications on desert development and Tibetan Plateau uplift in west China [J]. *Science in China Series D: Earth Sciences*, 45(4): 289–299.
- Filonchyk M. 2021. Characteristics of the severe March 2021 Gobi Desert dust storm and its impact on air pollution in China [J]. *Chemosphere*, 287: 132219. DOI: 10.1016/j.chemosphere.2021.132219.
- Han J, Dai H, Gu Z L. 2021. Sandstorms and desertification in Mongolia, an example of future climate events: a review [J]. *Environmental Chemistry Letters*, 19(6): 4063–4073.
- Han L, Hao Q Z, Qiao Y S, et al. 2019. Geochemical evidence for provenance diversity of loess in southern China and its implications for glacial aridification of the northern subtropical region [J]. *Quaternary Science Reviews*, 212: 149–163.
- Hao Q Z, Guo Z T, Qiao Y S, et al. 2010. Geochemical evidence for the provenance of Middle Pleistocene loess deposits in southern China [J]. *Quaternary Science Reviews*, 29(23/24): 3317–3326.
- He M Y, Zheng H B, Clift P D. 2013. Zircon U-Pb geochronology and Hf isotope data from the Yangtze River sands: implications for major magmatic events and crustal evolution in Central China [J]. *Chemical Geology*, 360/361: 186–203.
- Hou J Z, D'Andrea W J, Wang M D, et al. 2017. Influence of the Indian monsoon and the subtropical jet on climate change on the Tibetan Plateau since the Late Pleistocene [J]. *Quaternary Science Reviews*, 163: 84–94.
- Jia Y L, Lai Z P, Zhang J R, et al. 2012. Chronology and provenance of aeolian sediments from Poyang Lake area in the middle reaches of the Yangtze River in China [J]. *Quaternary Geochronology*, 10: 44–49.
- Jiang Q D, Hao Q Z, Peng S Z, et al. 2020. Grain-size evidence for the transport pathway of the Xiashu loess in northern subtropical China and its linkage with fluvial systems [J]. *Aeolian Research*, 46: 100613. DOI: 10.1016/j.aeolia.2020.100613.
- Lai Z P, Zhang W G, Chen X, et al. 2010. OSL chronology of loess deposits in East China and its implications for East Asian monsoon history [J]. *Quaternary Geochronology*, 5(2/3): 154–158.
- Li Y, Song Y G, Fitzsimmons K E, et al. 2020. Origin of loess deposits in the North Tian Shan piedmont, Central Asia [J]. *Palaeogeography, Palaeoclimatology, Palaeoecology*, 559: 109972. DOI: 10.1016/j.palaeo.2020.109972.
- Liang P, Chen B, Yang X P, et al. 2022. Revealing the dust transport processes of the 2021 mega dust storm event in northern China [J]. *Science Bulletin*, 67(1): 21–24.
- Liang Z W, Gao S, Hawkesworth C J, et al. 2018. Step-like growth of the continental crust in South China: evidence from detrital zircons in Yangtze River sediments [J]. *Lithos*, 320/321: 155–171.
- Liu F, Li G J, Chen J. 2014. U-Pb ages of zircon grains reveal a proximal dust source of the Xiashu loess, Lower Yangtze River region, China [J]. *Chinese Science Bulletin*, 59(20): 2391–2395.
- Nie J S, Peng W B, Möller A, et al. 2014. Provenance of the Upper Miocene-Pliocene Red Clay deposits of the Chinese Loess Plateau [J]. *Earth and Planetary Science Letters*, 407: 35–47.
- Nottebaum V, Stauch G, Hartmann K, et al. 2015. Unmixed loess grain size populations along the northern Qilian Shan (China): relationships between geomorphologic, sedimentologic and climatic controls [J]. *Quaternary International*, 372: 151–166.
- Pullen A, Kapp P, McCallister A T, et al. 2011. Qaidam Basin and northern Tibetan Plateau as dust sources for the Chinese Loess Plateau and paleoclimatic implications [J]. *Geology*, 39(11): 1031–1034.
- Qian P, Zheng X M, Cheng J, et al. 2018. Tracing the provenance of aeolian loess in the Yangtze River Delta through zircon U-Pb age and geochemical investigations [J]. *Journal of Mountain Science*, 15(4): 708–721.
- Qiao Y S, Hao Q Z, Peng S S, et al. 2011. Geochemical characteristics of the eolian deposits in southern China, and their implications for provenance and weathering intensity [J]. *Palaeogeography, Palaeoclimatology, Palaeoecology*, 308(3/4): 513–523.
- Rittner M, Vermeesch P, Carter A, et al. 2016. The provenance of Taklamakan desert sand [J]. *Earth and Planetary Science Letters*, 437: 127–137.
- Stevens T, Palk C, Carter A, et al. 2010. Assessing the

- provenance of loess and desert sediments in northern China using U-Pb dating and morphology of detrital zircons [J]. *Geological Society of America Bulletin*, 122(7/8): 1331–1344.
- Sun J M, Ding Z L, Xia X P, et al. 2018. Detrital zircon evidence for the ternary sources of the Chinese Loess Plateau [J]. *Journal of Asian Earth Sciences*, 155: 21–34.
- Sun Y B, Yan Y, Nie J S, et al. 2020. Source-to-sink fluctuations of Asian aeolian deposits since the Late Oligocene [J]. *Earth-Science Reviews*, 200: 102963. DOI: 10.1016/j.earscirev.2019.102963.
- Vermeesch P. 2012. On the visualisation of detrital age distributions [J]. *Chemical Geology*, 312/313: 190–194.
- Vermeesch P. 2018. IsoplotR: a free and open toolbox for geochronology [J]. *Geoscience Frontiers*, 9(5): 1479–1493.
- Waelbroeck C, Labeyrie L, Michel E, et al. 2002. Sea-level and deep water temperature changes derived from benthic foraminifera isotopic records [J]. *Quaternary Science Reviews*, 21(1/2/3): 295–305.
- Wang X Y, Lu H Y, Zhang H Z, et al. 2018. Distribution, provenance, and onset of the Xiashu loess in Southeast China with paleoclimatic implications [J]. *Journal of Asian Earth Sciences*, 155: 180–187.
- Windler G, Tierney J E, Anchukaitis K J. 2021. Glacial-interglacial shifts dominate tropical Indo-Pacific hydroclimate during the Late Pleistocene [J]. *Geophysical Research Letters*, 48(15): e2021GL093339. DOI: 10.1029/2021GL093339.
- Wu C, Zheng X M, Zhou L M, et al. 2021. Quantitative estimation of provenance contributions to loess deposits in Eastern China and implication for paleo-dust storm activity [J]. *Geomorphology*, 373: 107489. DOI: 10.1016/j.geomorph.2020.107489.
- Xie J, Yang S L, Ding Z L. 2012. Methods and application of using detrital zircons to trace the provenance of loess [J]. *Science China Earth Sciences*, 55(11): 1837–1846.
- Xie Y Y, Yuan F, Zhan T, et al. 2018. Geochemistry of loess deposits in northeastern China: constraint on provenance and implication for disappearance of the large Songliao palaeolake [J]. *Journal of the Geological Society*, 175(1): 146–162.
- Yin Z C, Wan Y, Zhang Y J, et al. 2021. Why super sandstorm 2021 in North China? [J]. *National Science Review*, 9(3): nwab165. DOI: 10.1093/nsr/nwab165.
- Yokoyama Y, Lambeck K, de Deckker P, et al. 2000. Timing of the Last Glacial Maximum from observed sea-level minima [J]. *Nature*, 406(6797): 713–716.
- Zhang H B, Nie J S, Liu X J, et al. 2021. Spatially variable provenance of the Chinese Loess Plateau [J]. *Geology*, 49(10): 1155–1159.
- Zhang H Z, Lu H Y, Xu X S, et al. 2016. Quantitative estimation of the contribution of dust sources to Chinese loess using detrital zircon U-Pb age patterns [J]. *Journal of Geophysical Research: Earth Surface*, 121(11): 2085–2099.
- Zhang Z, Jia Y L. 2019. Different provenance of separate loess sites in Yangtze River Basin and its paleoenvironmental implications [J]. *Journal of Mountain Science*, 16(7): 1616–1628.
- Zhu X Y, Liu L W, Wang X Y, et al. 2021. The Sr-Nd isotope geochemical tracing of Xiashu loess and its implications for the material transport mechanism of the Yangtze River [J]. *Catena*, 203: 105335. DOI: 10.1016/j.catena.2021.105335.